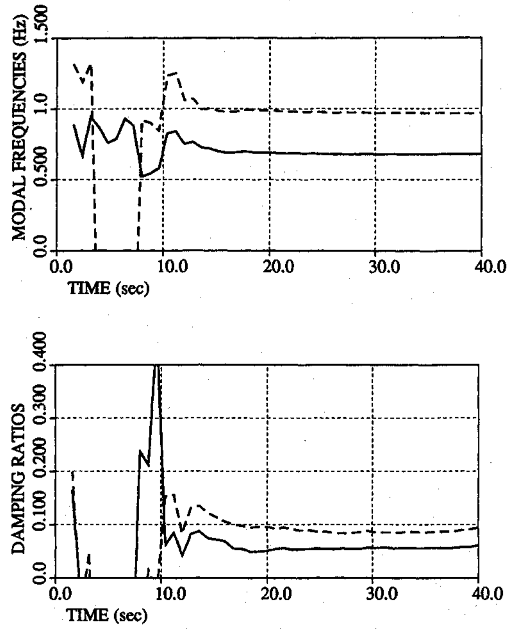

Fig. 4 System poles 4-input/1-output sensor X_1 (18th-order lattice).

algorithm, the two closely spaced modes can be progressively distinguished. Extraneous poles due to noise and/or nonlinearities are recognized by their erratic nature; whereas genuine system poles behave consistently.

Multi-Input System

For the multi-input time-invariant case, data are recorded while all four actuators are simultaneously excited. The input sequences are digital white noise bandlimited between 0.25 and 2 Hz sampled at 12.5 Hz in order to excite the low-frequency dynamics of the structure. The system poles are successively extracted for 4-input/1-output and 4-input/4-output configurations.

Sensor X_1 data are run through an 18th-order 4-input/1-output lattice filter. The resulting modal frequencies and damping ratios for sensor X_1 are shown in Fig. 4: one mode at 0.97 Hz with 0.09 damping and another mode at 0.68 Hz with 0.06 damping. Similar results, not shown, are obtained by running sensor Y_1 data through an 18th-order 4-input/1-output lattice filter: one mode at 0.97 Hz with 0.09 damping and one at 0.68 Hz with 0.09 damping. Structural analysis of the truss shows one torsional mode and two lateral modes, one along X and one along Y. Thus, sensor X_1 sees the torsional and X-lateral modes, and sensor Y_1 the torsional and Y-lateral modes. From the results, it can be deduced that the 0.97-Hz mode is the torsional mode since the damping is the same on both X_1 and Y_1, whereas the two lateral modes are at 0.68 Hz as proved by the difference in damping ratios. Previous single-input identification testing with lattice filters had not clearly revealed the existence of two modes at the same frequency. With a single actuator exciting the structure, the torsional and only one of the lateral modes are significantly excited (see Ref. 4 for results pertaining to this case). The multi-input excitation provides a richer picture of the system's dynamics.

The MIMO data are run through an 18th-order 4-input/4-output lattice. All sensors X_1, X_2, Y_1, and Y_2 are constrained to see the same dynamics. The outcome is a 0.97-Hz mode with 0.09 damping and a 0.68-Hz mode with 0.07 damping. The lattice filter has merged the two lateral modes into a single mode because it is not configured to separate X dynamics from Y dynamics. To ensure that both lateral modes are distinguished, the lattice should be set up so that X sensors (X_1, X_2) and Y sensors (Y_1, Y_2) observe different dynamics, in which case the a_i would be 2×2 matrices.

Conclusion

The vector-channel lattice filter was used to identify the truss experiment's modal frequencies and damping ratios for two important cases: a time-varying system with order change and a multi-input system configuration. The time-varying test was special in that the variation in parameters was significant as well as sudden, but, more importantly, the effective order of the system changed. The lattice filter adapted promptly to the parameter changes and was shown to detect order changes in the system. The multi-input data was found to give a better picture of system dynamics than single-input data, especially for the system damping ratios. These results suggest that the vector-channel lattice filter is an efficient on-line identification tool with applications in adaptive identification and control.

References

[1]Jabbari, F., and Gibson, J. S., "Vector Channel Lattice Filters and Identification of Flexible Structures," *IEEE Transactions on Automatic Control,* Vol. 33, No. 5, May 1988, pp. 448–456.

[2]Jabbari, F., and Gibson, J. S., "Adaptive Identification of Flexible Structures by Lattice Filters," *Journal of Guidance, Control, and Dynamics,* Vol. 12, No. 4, 1989, pp. 548–554.

[3]Lukich, M. S., "System Identification and Control of the Truss Experiment: A Retrospective," AIAA Paper 88-4152, Aug. 1988.

[4]Roesler, M. D., Jabbari, F., Lukich, M. S., and Gibson, J. S., "Identification of a Flexible Truss Structure Using Lattice Filters," *Proceedings of the American Control Conference,* Atlanta, GA, June 1988, American Automatic Control Council, Green Valley, AZ, pp. 1474–1482.

[5]Sundararajan, N., and Montgomery, R. C., "Identification of Structural Dynamics Systems Using Least-Squares Lattice Filters," *Journal of Guidance, Control, and Dynamics,* Vol. 6, No. 5, 1983, pp. 374–381.

[6]Sundararajan, N., and Montgomery, R. C., "Adaptive Modal Control of Structural Dynamics Systems Using Recursive Lattice Filters," *Journal of Guidance, Control, and Dynamics,* Vol. 8, No. 2, 1985, pp. 223–229.

[7]Wiberg, D. M., "Frequencies of Vibration Estimated by Lattices," *Journal of Astronautical Sciences,* Vol. 33, No. 1, 1985, pp. 35–47.

[8]Lee, D. T. L., "System Order Estimation of ARMA Models by Ladder Forms," *Proceedings of the American Control Conference,* American Automatic Control Council, Green Valley, AZ, 1983, pp. 1002–1007.

[9]Rissanen, J., "Modeling by Shortest Data Description," *Automatica,* Vol. 14, No. 5, 1978, pp. 465–471.

Dynamic Decrease of Drag by Optimal Periodic Control

Gottfried Sachs*
Technische Universität München, 8000 Munich 2, Germany

Introduction

RECENTLY, periodic cruise as opposed to the well-known steady-state cruise has acquired great interest since this type of an unsteady cruise offers a possibility for reducing the fuel consumption of aircraft. For a wide range of aircraft models, steady-state cruise is nonoptimal.[1] Numerical

Received Dec. 13, 1989; revision received April 7, 1990.

*Professor, Director of the Institute of Flight Mechanics and Flight Control. Associate Fellow AIAA.

results presented in the meantime give a quantitative indication of the fuel-consumption reduction that can be expected by applying optimal periodic control to aircraft cruise.[1-12]

In regard to the periodic cruise papers presented so far, an interesting problem partially solved is concerned with an aircraft model which has Mach-number-independent drag polar characteristics $C_D(C_L)$ and a specific fuel consumption σ proportional to speed V (or Mach number, respectively), i.e.,

$$C_D = C_{D_0} + KC_L^2 \tag{1a}$$

$$\dot{m}_f = \sigma T \tag{1b}$$

with $\sigma = \nu V$, where C_{D0}, K, and ν are constants. For such a type of an aircraft model, it has been shown that steady-state cruise is not optimal for supersonic or hypersonic Mach numbers above a certain threshold.[1] This velocity threshold is considered to be existent because of the need for substantial kinetic energy.[2] The question is why this threshold is affected by kinetic energy and whether there are conditions under which periodic cruise could be superior also at low speeds.

Besides its theoretical interest, the question raised may be of practical significance, too. This is because the fuel-consumption characteristics of propeller-driven aircraft are similar to Eq. (1b), and the speed range corresponds to the incompressible subsonic Mach number region. The fuel consumption of propeller-driven aircraft is related to propulsive power $P = TV$ such that $\dot{m}_f = \nu P$, where ν is a constant. This agrees with the model of Eq. (1b) according to $\dot{m}_f = \sigma T = \nu P$.

It is the purpose of this paper to present a solution for the problem addressed and to show that periodic cruise is optimal also at low speeds for the aircraft model under consideration. An additional purpose is to further develop the understanding of the physical mechanism underlying optimal periodic cruise. Thus, it will be shown that periodic control can produce a drag behavior the average of which is smaller than the minimum drag aerodynamically possible for steady-state cruise [equivalent to a flight at maximum lift drag ratio $(L/D)_{\max}$].

Problem Formulation and Optimization Procedure

Basically, the problem is to find optimal periodic flight paths where the fuel consumption per range is smaller than for the best steady-state cruise. This is equivalent to the periodic control problem consisting of minimizing the following performance criterion:

$$J = m_f(x_{cyc})/x_{cyc} \tag{2}$$

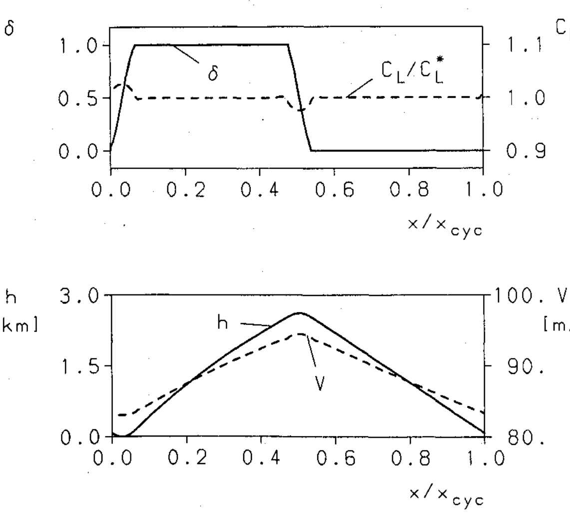

Fig. 1 Optimal cycle of periodic cruise, $(L/D)_{\max} = 15$, $P_{\max}/(mgV_0^*) = 0.17$, and $x_{cyc} = 82.6$ km [C_L^*: lift coefficient for (L/D) max].

where $m_f(x_{cyc})$ is the fuel consumed per range x_{cyc} representing the length of one cycle. The performance criterion is subject to the dynamic system (with the horizontal coordinate x used as independent variable)

$$\frac{dV}{dx} = \frac{T/m - D/m - g\sin\gamma}{V\cos\gamma}, \qquad \frac{d\gamma}{dx} = \frac{L/m}{V^2\cos\gamma} - \frac{g}{V^2}$$

$$\frac{dh}{dx} = \tan\gamma, \qquad \frac{dm_f}{dx} = \frac{\nu T}{\cos\gamma} \tag{3}$$

The mass of the aircraft can be considered constant since the fuel consumed in one cycle is small when compared with the total of the mass, i.e., $m_f(x_{cyc}) - m_f(0) \ll m$.

Flight-path periodicity and the initial fuel state yield the following boundary conditions:

$$V(x_{cyc}) = V(0), \qquad \gamma(x_{cyc}) = \gamma(0)$$

$$h(x_{cyc}) = h(0), \qquad m_f(0) = 0 \tag{4}$$

The thrust, lift, and drag force models are $T = \delta T_{\max}(V,h)$, $L = C_L(\rho/2)V^2S$, and $D = C_D(\rho/2)V^2S$, where C_D is given by Eq. (1a). The atmospheric model used is the ICAO standard atmosphere.[13]

Control variables are the lift coefficient and the throttle setting, which are subject to the following inequality constraints:

$$C_{L_{\min}} \le C_L \le C_{L_{\max}}, \qquad 0 \le \delta \le 1 \tag{5}$$

The optimization problem can now be stated as to find the control histories C_L and δ, the initial states $[V(0), \gamma(0), h(0)]$ and the periodic cycle length x_{cyc}, which minimize the performance criterion $J = m_f(x_{cyc})/x_{cyc}$ subject to Eqs. (3-5).

The optimization procedure applied uses necessary conditions based on the minimum principle. With the use of the Hamiltonian, Lagrange multipliers are adjoined to the equations of motion [Eq. (3)], thus yielding a system of eight differential equations.

In the numerical investigation, an optimization program based on the method of multiple shooting was applied.[14-16] In these references, the numerical procedure is described in detail.

Results and Underlying Physical Mechanism

In Fig. 1, the history of control and state variables for one cycle of an optimal periodic trajectory is presented, with data of a propeller-driven aircraft applied. Typically for optimal periodic cruise, a maximum-thrust increasing-energy condition is followed by a minimum-thrust decreasing-energy condition. Speed behavior is such that it shows higher values in the upper part of the trajectory, whereas the opposite holds for the lower part. This point will be addressed later in more detail when the underlying physical mechanism is discussed.

It may be of interest to note that speed stays at a rather low level throughout the whole trajectory. This is an indication that a velocity threshold may not exist.

Maximum power available and maximum lift/drag ratio have an effect on the improvement achievable with optimal periodic control. An evaluation of this effect is presented in Fig. 2, which shows the reduction in fuel consumption Δm_f. It will be shown later that Δm_f is equivalent to dynamic decrease of drag ΔD_{dyn}. From Fig. 2, it follows that a high power and a low lift/drag ratio level is favorable for the improvements resulting from optimal periodic control, However, the improvements are comparatively small.

The physical mechanism underlying the superiority of optimal periodic control and the nonexistence of a velocity threshold can be understood when considering the energy state management of the aircraft. Considering first the energy

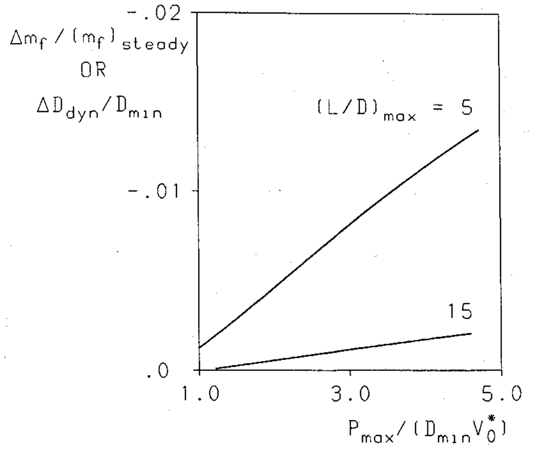

Fig. 2 Dynamic decrease of drag ΔD_{dyn} [D_{min}, $(m_f)_{steady}$: minimum values of drag and fuel consumption in steady-state cruise: V_0^* = speed for D_{min} at h = 0].

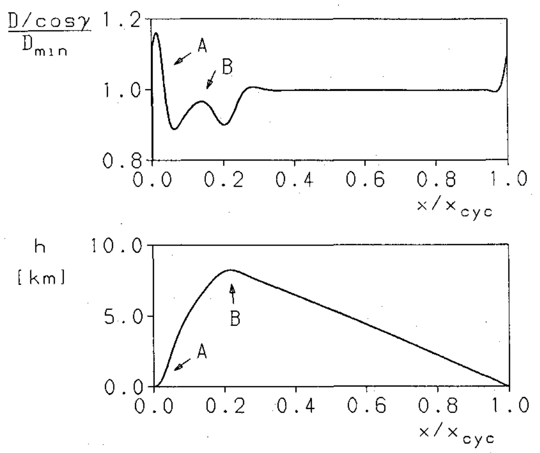

Fig. 3 Drag history for optimal periodic cruise as compared with minimum drag of steady-state cruise, $(L/D)_{max}$ = 15, $P_{max}/(mgV_0^*)$ = 0.62, and x_{cyc} = 194 km.

added to the aircraft energy state by the propulsion system, the following generally valid expression holds:

$$E_{add}(x) = \int_0^x \frac{T}{\cos\gamma}\,d\zeta \tag{6}$$

The fuel consumption written in a form also generally valid is given by

$$m_f = \int_0^t \dot{m}_f d\gamma = \int_0^t \sigma T d\gamma = \int_0^x \frac{\sigma T}{V\cos\gamma} d\zeta \tag{7}$$

Applying now the fuel-consumption model considered in this paper (i.e., $\sigma = \nu V$ where ν = const), the following expressions hold:

$$m_f(x) = \nu \int_0^x \frac{T}{\cos\gamma} d\zeta = \nu E_{add}(x)$$

or

$$\frac{E_{add}(x)}{m_f(x)} = \frac{1}{\nu} \neq f(V, h, \gamma, \delta) \tag{8}$$

This means that the energy added per fuel consumed is independent of speed, altitude, and throttle setting. In more general terms, it is independent of the state and control variables. As a result, no possibility exists for improving propulsion system efficiency by a special choice of V, h, γ, or δ. Therefore, an improvement achievable with periodic control must be completely due to a decrease of the energy subtracted from the aircraft energy state due to drag

$$E_{sub}(x) = \int_0^x \frac{D}{\cos\gamma} d\zeta \tag{9}$$

In fact, it can be shown that minimizing the performance criterion of Eq. (2), which is fuel consumed per range, is identical with minimizing $E_{sub}(x_{cyc})$ per range for the fuel-consumption model considered in this paper. From Eq. (8), it follows that

$$m_f(x_{cyc}) = \nu E_{add}(x_{cyc})$$

Since $E_{sub}(x_{cyc}) = E_{add}(x_{cyc})$ for the whole of a period, Eq. (9) may be used to give

$$m_f(x_{cyc}) = \nu E_{sub}(x_{cyc}) = \int_0^{x_{cyc}} \frac{D}{\cos\gamma} dx$$

Referring to Eq. (2), the performance criterion can now be expressed as

$$J = \frac{m_f(x_{cyc})}{x_{cyc}} = \frac{\nu}{x_{cyc}} \int_0^{x_{cyc}} \frac{D}{\cos\gamma} dx \tag{10}$$

As a result, minimizing fuel consumption is identical with minimizing $E_{sub}(x_{cyc})$. It may be of interest to note that the equality of minimizing fuel per range and minimizing the energy subtracted due to drag $E_{sub}(x_{cyc})$ only holds for the fuel-consumption characterisitics considered here. Usually, it is considered that there is a combination of different mechanisms for producing the superiority of periodic trajectories. Reference 6 provides more insight into such mechanisms and the conditions under which there are different effects existing.

From the results developed, it follows that drag can be decreased in a dynamic process by appropriately modulating speed, altitude, flight-path angle, and lift coefficient, $D = D(V, h, \gamma, C_L)$. As a consequence, the average of drag can be made smaller than the minimum of drag $D_{min} = mg/(L/D)_{max}$ aerodynamically possible in steady-state cruise. This effect is explored in more detail in the following.

In Fig. 3, the drag history during an optimal period is shown. In phase B, the drag is smaller than the minimum of drag in steady-state cruise D_{min} (actually, drag work per range $D/\cos\gamma$). The opposite is true for phase A. For the whole of a period, the drag decrease outweighs the drag increase. This is due to the fact that the drag decrease associated with the downward flight-path curvature (phase B in the lower part of Fig. 3) is larger than the drag increase in the upward flight-path curvature (phase A in the lower part of Fig. 3).

These drag changes are caused by the centrifugal force F_C associated with flight-path curvature, Fig. 4. The centrifugal force may be written as $F_C = mV\dot{\gamma} \approx mV^2\Delta\gamma/\Delta x$.

The drag change resulting may be expressed in linearized form as

$$\frac{\Delta D}{D_{min}} = \frac{V^2}{g}\frac{\Delta\gamma}{\Delta x} \tag{11}$$

From this expression, it follows that a negative flight-path curvature ($\Delta\gamma < 0$) at a higher speed produces a drag decrease which is larger than the drag increase resulting from a positive flight-path curvature ($\Delta\gamma > 0$) at a lower speed. This is the underlying mechanism that produces a drag decrease in a dynamic process by appropriate modulating speed, altitude, and lift.

It may be of interest to note that the effect described is due to relative changes in speed and not due to the absolute speed. Thus, the absolute speed level in terms of high speed (supersonic or hypersonic region) or low speed (subsonic region) is

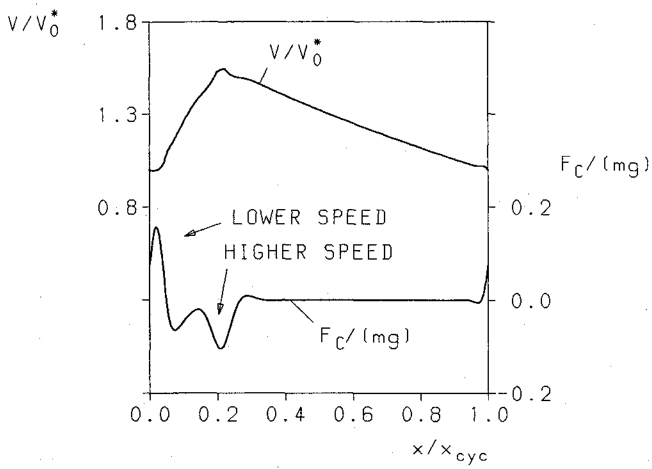

Fig. 4 Centrifugal force and corresponding speed and flight-path history.

qualitatively of no influence. As a consequence, a velocity threshold for the dynamic decrease of average drag is not existent.

Conclusions

Optimal periodic cruise is considered for aircraft whose thrust-specific fuel consumption is proportional to speed. It is shown that optimal periodic control of thrust and lift yields a decrease of the average of drag when compared with the minimum drag possible in steady-state flight. Numerical results for improvements are presented for a wide range of aircraft performance parameters, and the underlying physical mechanism for the dynamic decrease of drag is described.

References

[1]Speyer, J. L., "Nonoptimality of the Steady-State Cruise of Aircraft," *AIAA Journal,* Vol. 14, No. 11, 1976, pp. 1604–1610.

[2]Speyer, J. L., Dannemiller, D., and Walker, D., "Periodic Optimal Cruise of an Atmospheric Vehicle," *Journal of Guidance, Control, and Dynamics*, Vol. 8, No. 1, 1985, pp. 31–38.

[3]Gilbert, E. G., and Parsons, M. G., "Periodic Control and the Optimality of Aircraft Cruise," *Journal of Aircraft,* Vol. 13, No. 10, 1976, pp. 828–830.

[4]Grimm, W., Well, K.-H., and Oberele, H. J., "Periodic Control for Minimum Fuel Aircraft Trajectories," *Journal of Guidance, Control, and Dynamics*, Vol. 9, No. 2, 1986, pp. 169–174.

[5]Menon, P. K. A., "Study of Aircraft Cruise," *Journal of Guidance, Control, and Dynamics,* Vol. 12, No. 5, 1989, pp. 631–639.

[6]Breakwell, J. V., "Oscillatory Cruise—A Perspective," *Lecture Notes in Control and Information Sciences: Optimal Control*, edited by Burlisch, R., Miele, A., Stoer, J., Well, K. H., Springer-Verlag, Berlin, Vol. 95, 1987, pp. 157–168.

[7]Bhardwaj, P., Kelley, H. J., and Cliff, E. M. "Aircraft Cruise Performance Optimization Using Chattering Controls," *Proceedings of the 10th IFAC Congress*, International Federation of Automatic Control, Munich, 1987, pp. 200–205.

[8]Colonius, F., "Optimal Periodic Control," *Lecture Notes in Mathematics 1313*, Springer-Verlag, Berlin, 1988.

[9]Chuang, C.-H., Speyer, J. L., and Breakwell, J. V., "An Asymptotic Expansion for an Optimal Relaxation Oscillator," *SIAM Journal of Control and Optimization*, Vol. 726, No. 3, May 1988, pp. 678–696.

[10]Chuang, C.-H., and Speyer, J. L., "Periodic Optimal Hypersonic Scramjet Cruise," *Optimal Control Applications and Methods*, Vol. 8, No. 3, 1987, pp. 231–242.

[11]Sachs, G., and Christodoulou, T., "Endurance Increase by Cyclic Control," *Journal of Guidance, Control, and Dynamics*, Vol. 9, No. 1, 1986, pp. 58–63.

[12]Sachs, G., and Christodoulou, T., "Reducing Fuel Consumption of Subsonic Aircraft by Optimal Cyclic Cruise," *Journal of Aircraft*, Vol. 24, No. 9, 1987, pp. 616–622.

[13]ICAO Standard Atmosphere, International Civil Aviation Organization, Montreal, Canada, 1964.

[14]Bock, H. G., "Numerische Behandlung von Zustandsbeschränkten und Chebychef-Steuerungsproblemen," Course R1.06 of the Carl-Cranz-Gesellschaft, Oberpfaffenhofen, Germany, 1983.

[15]Oberle, H. J., "Numerische Berechnung optimaler Steuerungen von Heizung und Kühlung für ein realistisches Sonnenhausmodell," Institut für Mathemetik der Technischen Universität München, Munich, Germany, TUM-M8310, 1983.

[16]Bulirsch, R., "Die Mehrzielmethode zur Lösung von nichtlinearen Randwertproblemen und Aufgaben der optimalen Steuerung," Rept. of the Carl-Cranz-Gesellschaft, Oberfaffenhofen, Germany, 1971.